An Optimization Approach to the Frequency-Domain Inverse Problem for a Nonuniform LCRG Transmission Line

Martin Norgren and Sailing He

Abstract—**The inverse problem for a nonuniform LCRG transmission line is considered in the frequency domain. Imbedding equations for the reflection and transmission coefficients are derived through the concept of wave-splitting. An optimization approach is applied to reconstruct the line parameters as functions of the position using band-limited reflection and/or transmission data. Exact and explicit expressions for the gradients are derived, and the reconstruction algorithm (based upon a conjugate gradient method) is tested with both clean and noisy data. The problem of the nonuniqueness is also discussed.**

I. Introduction

Time-domain inverse problems for nonuniform transmission lines have been studied extensively recently by wave-splitting approaches [1], [2]. However, in many situations such as parameter reconstruction with band-limited data, design of filters, etc., it is of important to study the corresponding inverse problem in the frequency domain. The recent development and application of various optimization methods has proved their usefulness as efficient tools for obtaining various designs [3]–[5]. In the present paper, we apply an optimization approach to the reconstruction of the line parameters using the band-limited reflection and/or transmission data in the frequency-domain.

In the present paper, the direct solver is obtained by solving the imbedding equations for the reflection and transmission coefficients, which are derived through the concept of wave-splitting [6], [7]. To apply an optimization approach to an inverse problem, one introduces a suitable objective functional first, and then computes the gradient of this functional. In the present paper, we derive an exact and explicit expression for the gradient by introducing some auxiliary functions. The line parameters are then reconstructed by an iterative algorithm (based on the conjugate gradient method).

II. Problem Formulation and the Direct Solver

Consider a nonuniform transmission line occupying the region $x \in [0, l]$ where the parameters L (the inductance), C (the capacitance), R (the resistance) and G (the shunt conductance) varies with the position x. The telegrapher's equations for the voltage $V(x;\omega)$ and current $I(x;\omega)$ with harmonic time dependence $\exp(j\omega t)$ are

$$\frac{d}{dx}\begin{bmatrix} V \\ I \end{bmatrix} = \begin{bmatrix} 0 & -R - j\omega L \\ -G - j\omega C & 0 \end{bmatrix}\begin{bmatrix} V \\ I \end{bmatrix} \equiv \boldsymbol{D}\begin{bmatrix} V \\ I \end{bmatrix}. \tag{1}$$

The nonuniform line is excited at $x = 0$ from a uniform (not necessarily lossless) transmission line with a characteristic impedance Z_0, and is terminated with a load impedance Z_L at $x = l$. Note that both Z_0 and Z_L may be in general frequency-dependent. The inverse problem is to determine one or several of the line parameters in the region $[0, l]$ from the reflection and/or transmission data in a certain frequency band (in all the numerical examples in the present paper, we use scattering data in a microwave frequency band). To enhance the input information for reconstruction, we may also use the reflection data at $x = l$ when the line is excited at $x = l$ (right-sided excitation). However, to simplify the notation we will only give the formulas and their derivations for the left-sided excitation, since the formalism is completely analogous for the right-sided excitation.

To apply an optimization approach, one needs a direct solver for the direct problem to calculate the gradient at each iteration. In this section we derive the imbedding equations for the reflection and transmission coefficients through the concept of wave-splitting, and use them as the direct solver. We use the following wave-splitting [7]

$$\begin{bmatrix} V^+ \\ V^- \end{bmatrix}(x;\omega) = \frac{1}{2}\begin{bmatrix} 1 & Z_0 \\ 1 & -Z_0 \end{bmatrix}\begin{bmatrix} V \\ I \end{bmatrix}(x;\omega) \equiv \boldsymbol{T}_0\begin{bmatrix} V \\ I \end{bmatrix}(x;\omega). \tag{2}$$

Note that $V^+(x;\omega)$ and $V^-(x;\omega)$ are the incident and reflected voltages, respectively, in the homogeneous region $x \le 0$. Using (1) and (2), one obtains the following system of equations for the split voltages

$$\frac{d}{dx}\begin{bmatrix} V^+ \\ V^- \end{bmatrix} = \boldsymbol{T}_0\boldsymbol{D}\boldsymbol{T}_0^{-1}\begin{bmatrix} V^+ \\ V^- \end{bmatrix} \equiv \begin{bmatrix} -a & -b \\ b & a \end{bmatrix}\begin{bmatrix} V^+ \\ V^- \end{bmatrix} \tag{3}$$

where

$$a = \tfrac{1}{2}[j\omega(CZ_0 + LZ_0^{-1}) + (GZ_0 + RZ_0^{-1})], \tag{4}$$

$$b = \tfrac{1}{2}[j\omega(CZ_0 - LZ_0^{-1}) + (GZ_0 - RZ_0^{-1})]. \tag{5}$$

The reflection and transmission coefficients for the nonuniform transmission line can be determined by an invariant imbedding method. In this method one considers an imbedding geometry, i.e., a subline $[x, l]$ of the original line $[0, l]$, and assumes that the subline is temporarily terminated at the left side with a uniform line with a charactaristic impedance Z_0. For this *imbedding geometry*, the reflection coefficient (denoted $r(x;\omega)$) and the transmission coefficient (denoted $t(x;\omega)$) are defined as follows

$$V^-(x;\omega) = r(x;\omega)V^+(x;\omega), \tag{6}$$

$$V(l;\omega) = t(x;\omega)V^+(x;\omega). \tag{7}$$

From the above definitions one sees that $r(0;\omega), t(0;\omega)$ are the physical reflection and transmission coefficients, respectively, for the original nonuniform line. From (3) and (6), one can obtain the following imbedding equation for $r(x;\omega)$

$$\frac{d}{dx}r = 2ar + b(1 + r^2) \tag{8}$$

together with the boundary condition

$$r(l;\omega) = \frac{Z_L - Z_0}{Z_L + Z_0}. \tag{9}$$

By integrating (8) in the $-x$ direction (starting from $x = l$), one can obtain the reflection coefficient for the original nonuniform line, i.e. $r(0;\omega)$. Similarly, one can obtain the following linear imbedding equation for $t(x;\omega)$,

$$\frac{d}{dx}t = (a + br)t \tag{10}$$

together with the following boundary condition

$$t(l;\omega) = \frac{2Z_L}{Z_L + Z_0}. \tag{11}$$

Manuscript received August 22, 1995; revised April 19, 1996. This work was supported in part by the Swedish Research Council for Engineering Sciences.

The authors are with the Department of Electromagnetic Theory Royal Institute of Technology, S-100 44 Stockholm, Sweden.

Publisher Item Identifier S 0018-9480(96)05646-3.

III. An Optimization Approach

Introduce a four-element parameter vector $p = (L, C, R, G)^T$ (the superscript T denotes the transposition). Define an objective functional as follows:

$$J(p) = \sum_{\omega=\omega_{\min}}^{\omega_{\max}} w_r(\omega)|r(0;\omega) - r_m(\omega)|^2 + w_t(\omega)|t(0;\omega) - t_m(\omega)|^2 \tag{12}$$

where $r_m(\omega), t_m(\omega)$ are the *measured* reflection and transmission coefficients, respectively, and $w_r(\omega), w_t(\omega)$ are weighting functions (nonnegative) describing the weight of using the reflection and transmission data at different frequency points. In the above definition, the summation is performed over discrete frequency points in a certain frequency band $[\omega_{\min}, \omega_{\max}]$. Note that one important reason for choosing the L_2-norm in the present paper is that this choice makes it possible to derive exact expressions for the gradient of $J(p)$ (if one computes the gradient by numerical perturbations, then L_1-norm is efficient for use [4], however, the computation will be one order slower than the one using the present analytical gradient, see Section 4.2 below).

A. Explicit Expression for the Gradient

Let $\tilde{r} = r(x; p + \delta p)$ and $\tilde{t} = t(x; p + \delta p)$ be the solutions to (8)–(11) with the parameter vector $p + \delta p$. Then $\delta r \equiv \tilde{r} - r$ and $\delta t \equiv \tilde{t} - t$ satisfy the following system of equations and boundary conditions:

$$\frac{d}{dx}\begin{bmatrix}\delta r \\ \delta t\end{bmatrix} - \begin{bmatrix}2(a+br) & 0 \\ bt & a+br\end{bmatrix}\begin{bmatrix}\delta r \\ \delta t\end{bmatrix} = \begin{bmatrix}2r\delta a + (1+r^2)\delta b \\ t(\delta a + r\delta b)\end{bmatrix} + o(\delta p), \tag{13}$$

$$\delta r(l) = \delta t(l) = 0 \tag{14}$$

where

$$\delta a = a(p+\delta p) - a(p), \delta b = b(p+\delta p) - b(p)$$

and

$$\lim_{\|\delta p\| \to 0} \frac{o(\delta p)}{\|\delta p\|} = 0$$

($\| \|$ denotes the L_2 norm, i.e., $\|f(x)\| = \{\int_0^l |f(x)|^2\, dx\}^{1/2}$).

The corresponding increment of the functional $J(p)$ can then be written as follows:

$$\begin{aligned}\delta J(p) &\equiv J(p+\delta p) - J(p) \\ &= 2\Re e \sum_{\omega=\omega_{\min}}^{\omega_{\max}} \{w_r[r(0;\omega) - r_m(\omega)]^* \delta r(0;\omega) \\ &\quad + w_t[t(0;\omega) - t_m(\omega)]^* \delta t(0;\omega)\} + o(\delta p)\end{aligned} \tag{15}$$

where the superscript $*$ denotes the complex conjugate, and $\Re e$ denotes the real part. Introduce a pair of auxiliary functions $U(x;\omega)$ and $W(x;\omega)$ which satisfy the following system of equations and boundary conditions

$$\frac{d}{dx}\begin{bmatrix}U \\ W\end{bmatrix} + \begin{bmatrix}2(a+br) & bt \\ 0 & a+br\end{bmatrix}\begin{bmatrix}U \\ W\end{bmatrix} = 0 \tag{16}$$

$$U(0;\omega) = w_r(\omega)[r(0;\omega) - r_m(\omega)]^*, \tag{17}$$

$$W(0;\omega) = w_t(\omega)[t(0;\omega) - t_m(\omega)]^*. \tag{18}$$

The increment in the functional can thus be written as

$$\delta J(p) = 2\Re e \sum_{\omega=\omega_{\min}}^{\omega_{\max}} \{U(0;\omega)\delta r(0;\omega) + W(0;\omega)\delta t(0;\omega)\} + o(\delta p). \tag{19}$$

From (13) and (16), one has

$$\frac{d}{dx}(U\delta r + W\delta t) = (2r\delta a + (1+r^2)\delta b)U + (\delta a + r\delta b)tW + o(\delta p) \tag{20}$$

which gives (cf. the boundary condition (14))

$$\begin{aligned}U(0;\omega)\delta r(0;\omega) + W(0;\omega)\delta t(0;\omega) &= -\int_0^l \{(2r\delta a + (1+r^2)\delta b)U \\ &\quad + (\delta a + r\delta b)tW\}\, dx + o(\delta p).\end{aligned} \tag{21}$$

From (10) and (16) it immediately follows that $(d/dx)(tW) = 0$, i.e., $t(x;\omega)W(x;\omega) \equiv K(\omega)$, where [cf. (18)]

$$K(\omega) \equiv w_t(\omega)[t(0;\omega) - t_m(\omega)]^* t(0;\omega). \tag{22}$$

Therefore, one can write the increment of the functional as

$$\delta J(p) = -2\int_0^l dx\, \Re e \sum_{\omega=\omega_{\min}}^{\omega_{\max}} \{[2r\delta a + (1+r^2)\delta b]U + (\delta a + r\delta b)K\} + o(\delta p). \tag{23}$$

If all the line parameters are nondispersive, one can rewrite (23) in an inner product form

$$\begin{aligned}\delta J(p) &= \int_0^l g^T \cdot \delta p\, dx + o(\delta p) \\ &\equiv \langle g_L, \delta L\rangle + \langle g_C, \delta C\rangle \\ &\quad + \langle g_R, \delta R\rangle + \langle g_G, \delta G\rangle + o(\delta p)\end{aligned} \tag{24}$$

where $g(x)$ is the gradient of the objective functional. Using (4) and (5) to express the increments δa and δb in (23) in terms of the parameter increments, one can identify the gradients as

$$g_L(x) = -\Re e \sum_{\omega=\omega_{\min}}^{\omega_{\max}} j\omega[Z_0(\omega)]^{-1} \cdot \{K(\omega)(1 - r(x;\omega)) - (1 - r(x;\omega))^2 U(x;\omega)\}, \tag{25}$$

$$g_C(x) = -\Re e \sum_{\omega=\omega_{\min}}^{\omega_{\max}} j\omega Z_0(\omega) \cdot \{K(\omega)(1 + r(x;\omega)) + (1 + r(x;\omega))^2 U(x;\omega)\}, \tag{26}$$

$$g_R(x) = -\Re e \sum_{\omega=\omega_{\min}}^{\omega_{\max}} [Z_0(\omega)]^{-1} \cdot \{K(\omega)(1 - r(x;\omega)) - (1 - r(x;\omega))^2 U(x;\omega)\}, \tag{27}$$

$$g_G(x) = -\Re e \sum_{\omega=\omega_{\min}}^{\omega_{\max}} Z_0(\omega) \cdot \{K(\omega)(1 + r(x;\omega)) + (1 + r(x;\omega))^2 U(x;\omega)\}. \tag{28}$$

Note that if the scattering data for right-sided excitation, as well as the the scattering data for left-sided excitation, are used in an

inverse problem, an analogous term should be added in the definition (12) of the objective functional. Consequently in that case the above expressions for the gradients will be modified with additional terms [which are similar to the righthand side expressions of (25)–(28)].

IV. Numerical Reconstruction

A. Reconstruction of One Parameter from One-Sided Reflection Data

Example 1: In this numerical example we consider a transmission line with a piecewise constant conductance as shown by the solid line in Fig. 1(a) (the length of the line is $l = 0.2$ m). The other three parameters are constant with values of $L = 0.50\ \mu\text{H/m}, C = 50\ \text{pF/m}$ and $R = 0\ \Omega/\text{m}$. The nonuniform line is terminated at $x = 0$ with a uniform line with a characteristic impedance $Z_0 = 50\ \Omega$. The load end (at $x = 0.2$ m) is left open, i.e. $Z_L = \infty$. For a line with piecewise constant parameters, one can easily obtain an explicit solution for the reflection coefficient by using recursively the following formula [11]

$$Z_{\text{in}} = Z_{\text{char}} \frac{Z_{\text{load}} + Z_{\text{char}} \tanh(\gamma d)}{Z_{\text{char}} + Z_{\text{load}} \tanh(\gamma d)} \tag{29}$$

for each subportion of the line, starting at $x = l$. In (29)

$$\gamma = \sqrt{(R + j\omega L)(G + j\omega C)},$$
$$Z_{\text{char}} = \sqrt{(R + j\omega L)/(G + j\omega C)}$$

d is the length of the subportion, and Z_{in} is the input impedance of the subportion when its load impedance is Z_{load}. When $Z_{\text{in}}|_{x=0}$ is calculated, the reflection coefficient can be obtained by $r_m(\omega) = [Z_{\text{in}}|_{x=0} - Z_0]/[Z_{\text{in}}|_{x=0} + Z_0]$. The calculated reflection coefficient $r_m(\omega)$ in the frequency band $f \in [10\ \text{MHz}, 10\ \text{GHz}]$ is shown in Fig. 1(b), and will be used as the measured reflection data for the inverse problem in this example. Since the input data $r_m(\omega)$ is calculated in a way that is different from the direct solver, the numerical "marching back effect" can be avoided when solving the inverse problem. 201 frequency points are used with a logarithmic spacing in the microwave frequency band $f \in [10\ \text{MHz}, 10\ \text{GHz}]$, and 401 grid-points are used in $x \in [0, l]$. In this example we choose the weighting function for the reflection data as $w_r(\omega) = 100^{-(\omega/\omega_{\max})^2}$, where $\omega_{\max} = 2\pi \cdot 10^9\ \text{s}^{-1}$ (see the dotted line in Fig. 1(b); $w_t(\omega) \equiv 0$, i.e., no transmission data is used). The dashed line in Fig. 1(a) is the reconstruction after 150 iterations (the starting guess is identically zero). To test the stability of the algorithm, Gaussian noise with a standard deviation $\sigma = 0.05 \cdot \max|r_m(\omega = 2\pi f)|$ is added on both the real and the imaginary parts of $r_m(\omega)$ [see the dashed lines in Fig. 1(b)]. The dotted line in Fig. 1(a) is the corresponding reconstruction using the noisy reflection data. The influence of noise is clearly visible around $x = 0.16$ m where the parameter has a large discontinuity. Nevertheless, one sees from this figure that the reconstruction algorithm is reasonably stable (the reconstruction algorithm is more stable if the parameter has a smooth continuous profile). One may reduce the sensitivity of the algorithm to the noise in the reconstruction of a discontinuous parameter by certain type of regularization (e.g., Tikhonov type [9]).

In the case of reconstructing one parameter, we found that any of the parameters L, C, R and G can be successfully reconstructed from one-sided reflection data. If two-sided reflection data are used, the speed of convergence can be increased significantly. The inclusion of transmission data does not give any improvement of the reconstruction (see the Section IV-D below).

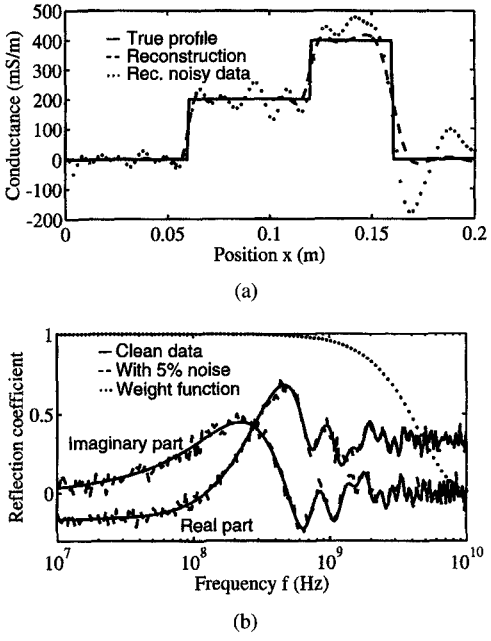

Fig. 1. (a) Reconstruction of the shunt conductance $G(x)$. (b) The reflection coefficient.

B. Reconstruction of Two Parameters from Two-Sided Reflection Data

Our numerical experiments indicate that using only one-sided excitation we cannot obtain a good simultaneous reconstruction of two parameters (the other two are assumed to be known) with the optimization approach. However, when two-sided reflection data are used, we can reconstruct two parameters simultaneously. The reconstruction of a reactive parameter (L or C) together with a dissipative parameter (R or G) appears to be successful with a fast convergence. Reconstruction of the two dissipative parameters, R and G, is also successful. In the case of reconstructing the two reactive parameters L and C, the reconstruction is successful (however, with a slow convergence) if the nonuniform line is lossy. If $R = G \equiv 0$, unsuccessful reconstruction readily occurs, which is consistent with a time-domain numerical experiment given in [2].

Example 2–A Dispersive Case: The telegrapher's equations (1) are derived with the assumption that the wave in the transmission line is (or approximately is) a TEM-wave, which is true only for the case when the conductivity σ_c of the conductors is much higher than the conductivity σ of the material between the conductors. In such a case, the series resistance R at high frequencies is proportional to the real part of the surface impedance Z_s, which is given by $Z_s = (1 + j)\sqrt{\omega\mu_c/2\sigma_c}$ (μ_c is the permeability of the conductors, see [10]). The imaginary part of Z_s is due to an *internal* inductance L_i. In view of this physical background we consider a dispersive case for which R in the telegrapher's equations (1) is replaced with the following quantity

$$R(x, \omega) + j\omega L_i(x, \omega) \equiv (1 + j)Q(x)\sqrt{\omega} \tag{30}$$

where $Q(x)$ is proportional to $\sqrt{\mu_c(x)/\sigma_c(x)}$ [11]. Consequently, the expression (27) for the gradient $g_R(x)$ should be replaced with the following expression for the gradient with respect to the function $Q(x)$

$$g_Q(x) = -\Re e \sum_{\omega=\omega_{\min}}^{\omega_{\max}} (1 + j)\sqrt{\omega} Z_0^{-1}(\omega) \cdot \{K(\omega)(1 - r(x; \omega)) - (1 - r(x; \omega))^2 U(x; \omega)\}. \tag{31}$$

As a numerical example, we choose the length of the nonuniform line as $l = 0.2$ m. The nonuniform dispersive line is always excited from a 50 Ω uniform LC-line and kept open at the other end (i.e., the load impedance is $Z_L = \infty$), for both cases of the left- and right-sided reflection. The line parameters are chosen as shown by the solid lines in Figs. 2–4. The number of gridpoints in x is 101, and 30 frequency points are used over the frequency band $f \in$ [50 MHz, 1.5 GHz] with a linear spacing. The measured reflection coefficient $r_m(\omega)$ is calculated by solving the imbedding equation (8) together with the boundary condition (9). We choose the starting guess of the line parameters as $L = 0.25\ \mu$H/m, $C = 100$ pF/m, $R = 0$, and $G = 0$.

The dashed lines in Fig. 2 are the simultaneous reconstruction of L and R (at the frequency 500 MHz; note that the reconstruction is carried out for the parameter pairs $L(x)$ and $Q(x)$, although the reconstruct result is shown for L and $R \equiv Q\sqrt{\omega}$ in Fig. 2) after 60 iterations. We have also compared the CPU times and the accuracy between the reconstructions obtained with and without the analytical gradients for this example. When an analytical gradient is not available, one can calculate the gradient numerically through the following series of step functions

$$\psi_i(x) = \begin{cases} 1, & x_{i-1} \le x \le x_i, \\ 0, & \text{otherwise} \end{cases}$$

where $x_i, i = 1, 2, \cdots, N$, are the discretized positions. Assume that $P(x) = \Sigma_i\ P_i\psi_i(x)$($P(x)$ is a parameter to be reconstructed), and the corresponding gradient $g(x) = \Sigma_i\ g_i\psi_i(x)$, then one can calculate the coefficient g_i numerically by a small perturbation as shown at the bottom of the page where ϵ is a small quantum. In the present reconstruction algorithm, the computation time is mainly consumed by calling the direct solver (i.e., solving the imbedding equations for r and t), and the auxiliary direct solver (i.e., solving the differential equations for the auxiliary functions) which takes a roughly equal time as the direct solver. To calculate the gradient, one has to call the direct solver N times when the numerical perturbation is used, while using the present analytical expression one only needs to call the direct solver and the auxiliary direct solver once. Therefore, the ratio of the computation times for the gradient between with and without the analytical expression is about $2/N$. In fact the ratio of the overall computation time for the reconstruction (if same number of iterations is required) between with and without the analytical gradients is about $2 + n_s/n_pN + 1 + n_s$, where n_p is the number of the parameters to be reconstructed (in a two-parameter reconstruction case, $n_p = 2$), and n_s is the average number of steps in the line search within each iteration ($n_s \approx 2$ if an optimal line search program is used). This has been verified numerically. When $N = 101$, and the number of frequency points is 20, the time for calculating the gradient is about six seconds when the analytical expressions are used, but is ten minutes when a small numerical perturbation is used (the programs are run on a Macintosh computer of MC68040 type). The overall computation time for the reconstruction (after 18 iterations) is about seven minutes when the analytical gradients are used, while it takes three hours and twenty minutes when the gradients are calculated by small numerical perturbation (with same number of iterations; the reconstruction result is certainly worse than the one obtained with the analytical gradients). This is consistent with the observed value $n_s \approx 5.6$ (we have not used an optimal line search program in our reconstruction code; the difference in overall CPU times will be more significant if an optimal line search program is used).

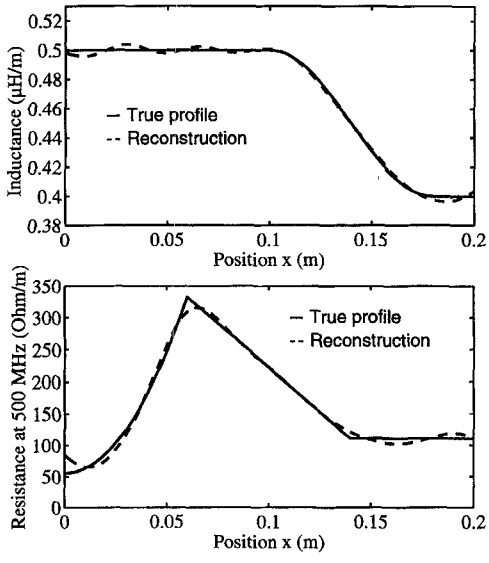

Fig. 2. Simultaneous reconstruction of the inductance L and the resistance R (dispersive).

The simultaneous reconstruction of R (at the frequency 500 MHz) and G using two-sided reflection data is shown by the dashed lines in Fig. 3 after 100 iterations. The simultaneous reconstruction of L and C is presented in Fig. 4 after 100 iterations. The dashed lines in Fig. 4 give the simultaneous reconstruction when the nonuniform line is lossy (with R and G as shown by the solid lines in Fig. 3), while the dotted lines are the corresponding reconstruction when the nonuniform line is lossless (i.e., $R = G = 0$). The reconstruction is reasonably good in the lossy case, but fails in the lossless case. Numerical experiments indicated that in the case of reconstructing L and C when the line is lossless, the failure lies in the reconstruction of the wave-front velocity $(LC)^{-1/2}$ (the reconstruction of the characteristic impedance $(L/C)^{1/2}$ is still reliable).

C. Reconstruction of More Than Two Parameter

For simultaneous reconstruction of three parameters, we examined the simultaneous reconstruction of G, R, and one of L and C, which is expected to be the easiest case. Successful reconstruction using two-sided reflection data can be achieved only when the starting guess of the line parameters is close to their true parameter profiles (otherwise the reconstruction readily fails). Numerical experiments also show that using several different values for the load impedance Z_L does not give any improvement in the reconstruction.

D. The Use of Transmission Data

The solution to the inverse problem of reconstructing any line parameter using only transmission data is in general not unique. For example, if the load impedance is equal to the impedance of the terminated uniform line, i.e., $Z_L = Z_0$, it can be shown from two-port theory that it is impossible to distinguish a parameter profile $p(x)$ from its center-image profile $p(l-x)$, when only transmission data is used (i.e., the two profiles generate the same transmission data). Even

$$g_i \approx \frac{J(\langle P_0, P_1, \cdots, P_i + \epsilon, \cdots, P_N\rangle) - J(\langle P_0, P_1, \cdots, P_i, \cdots, P_N\rangle)}{\epsilon}$$

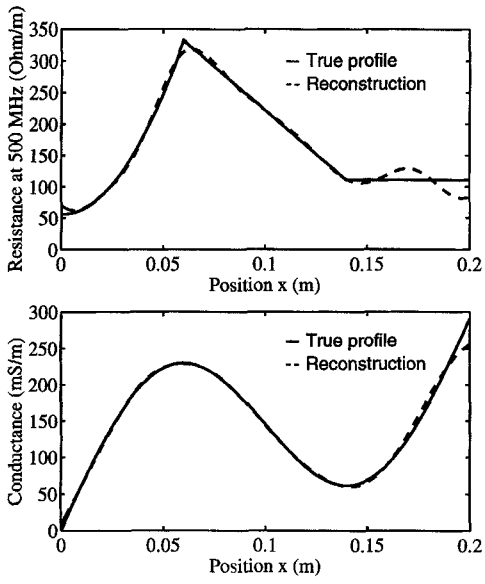

Fig. 3. Simultaneous reconstruction of the resistance R (dispersive) and the conductance G.

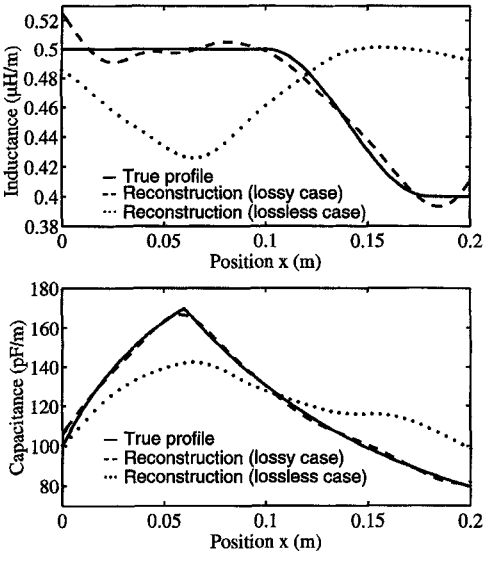

Fig. 4. Simultaneous reconstruction of the inductance L and the capacitance C.

when the solution to the inverse problem is unique, the reconstruction may not be achieved due to the existence of local minima.

In the previous subsections, we used only reflection data in the numerical reconstruction, and we never came across a case in which the reconstruction was trapped by a local minimum, i.e., it appears that the objective functional, defined by (12) with $w_t \equiv 0$, is convex in a very large area centered at the true profile. One may like to include the transmission data to make full use of the available information. However, our numerical experiments show that including the transmission data will introduce local minima, and thus it is better not to use the transmission data at all in the present optimization approach.

V. Conclusion

In the present paper, we have described an optimization approach to the frequency-domain inverse problem for a nonuniform $LCRG$ line. Imbedding equations for the reflection and transmission coefficients have been given, and the exact and explicit expressions for the gradients have been derived. The reconstruction algorithm have been tested with both clean and noisy data. Numerical results have shown that any single parameter can be reconstructed from one-sided reflection data, and various pairs of parameters can be reconstructed simultaneously from two-sided reflection data. Several other aspects have been discussed, including simultaneous reconstruction of more than two parameters, and the use of the transmission data.

Acknowledgment

The authors would like to thank J. Lundstedt for valuable discussions.

References

[1] S. He and S. Ström, "Time domain wave splitting approach to transmission along a nonuniform LCRG line," *J. Electromagn. Waves Applicat.*, vol. 6, no. 8, pp. 995–1014, 1992.

[2] J. Lundstedt and S. Ström, "Simultaneous reconstruction of two parameters from the transient response of a nonuniform LCRG transmission line," *J. Electromagn. Waves Applicat.*, vol. 10, no. 1, pp. 19–50, 1996.

[3] R. K. Brayton, G. D. Hachtel, and A. L. Sangiovanni-Vincentelli, "A survey of optimization techniques for integrated-circuit design," *Proc. IEEE*, vol. 69, pp. 1334–1362, 1981.

[4] J. W. Bandler, S. H. Chen, and S. Daijavad, "Microwave device modeling using efficient l_1 optimization: a novel approach," *IEEE Trans. Microwave Theory Tech.*, vol. MTT-34, pp. 1282–1293, 1986.

[5] J. J. Pesque, D. P. Bouche, and R. Mittra, "Optimization of multilayer antireflection coatings using an optimal control method," *IEEE Trans. Microwave Theory Tech.*, vol. 40, pp. 1789–1796, 1992.

[6] S. He, "A time-harmonic Green function technique and wave propagation in a stratified nonreciprocal chiral slab with multiple discontinuities," *J. Math. Phys.*, vol. 33, no. 12, pp. 4103–4110, 1992.

[7] M. Norgren and S. He, "A general scheme for the electromagnetic reflection and transmission for composite structures of complex media," *Proc. IEE, Part H: Microwaves, Antennas Propagat.*, vol. 142, no. 1, pp. 52–56, 1995.

[8] E. Polak, *Computational methods in optimization.* New York and London: Academic, 1971, p. 306.

[9] C. W. Groetsch, *The Theory of Tikhonov Regularization for Fredholm Equations of the First Kind*, Research Notes in Mathematics. New York: Pitman, 1984.

[10] J. D. Jackson, *Classical Electrodynamics.* New York: Wiley, sec. 8.1, 1975.

[11] D. K. Cheng, *Fundamentals of Engineering Electromagnetics.* Reading, MA: Addison-Wesley, 1993.